

# 15463 Final Project: 3D Structured Light with XOR, Binary, Gray Codes

3 RUSLANA FOGLER, Carnegie Mellon University

5 Three-Dimensional Structured Light is a method used to reconstruct point  
6 clouds of a 3D scene by relying on matching correspondences between a  
7 camera and a projector. This process is highly advantageous for recon-  
8 structing stationary scenes because it is more efficient point matching  
9 than conventional stereo vision with two cameras, because of rapid and  
10 cost-effective data capture, and because it can be reused to develop more  
11 scenes after the calibration is completed. By using binary or gray codes,  
12 the number of images required to create point correspondences is reduced  
13 to  $\lfloor \log_2 \text{Number of Column Pixels} \rfloor$ , but the results are also susceptible to  
14 subsurface light scattering and interreflections. Instead, another approach is  
15 using XOR codes, which are more robust to the aforementioned phenomena.  
16 In my 15463 final project, I implemented a 3D Structured Light project that  
17 supports binary, gray, and XOR codes.

18 Additional Key Words and Phrases: Camera Calibration, Projector Calibra-  
19 tion, Structured Light, Stereo Vision, 3D Reconstruction

## 20 ACM Reference Format:

21 Ruslana Fogler. 2025. 15463 Final Project: 3D Structured Light with XOR,  
22 Binary, Gray Codes. *ACM Trans. Graph.* 1, 1 (December 2025), 5 pages. <https://doi.org/10.1145/nnnnnnn.nnnnnnn>

24 float

## 26 1 INTRODUCTION

### 28 1.1 3D Structured Lighting Background

29 Since the late 20th century, 3D Structured Light has gained traction  
30 as being an efficient, relatively cheap, and highly accurate way to  
31 construct a 3D visualization of a scene. This growth has culminated  
32 in efforts such as the Digital Michelangelo Project [1], enormous  
33 amounts of research, and applications to industries such as manu-  
34 facturing, healthcare, cultural preservation, etc. To use the method,  
35 a user must set up a light projector and a camera pair to face a scene.  
36 The light projector is made to shine a number of certain known  
37 patterns on a scene—typically in the form of column stripes. The  
38 camera is used in tandem to capture images.

39 With the acquired image data, the user can extract row/column  
40 correspondences from the illuminated scenes. If the camera and  
41 projector's intrinsic and extrinsic parameters are known, they can  
42 be used to form a stereo pair, and the decoded row/columns serve  
43 as epipolar point correspondence. By back-projecting rays and per-  
44 forming triangulation, the depth of a scene can be recovered.

---

46 Author's address: Ruslana Fogler, rfogler@andrew.cmu.edu, Carnegie Mellon University.

49 Permission to make digital or hard copies of all or part of this work for personal or  
50 classroom use is granted without fee provided that copies are not made or distributed  
51 for profit or commercial advantage and that copies bear this notice and the full citation  
52 on the first page. Copyrights for components of this work owned by others than the  
53 author(s) must be honored. Abstracting with credit is permitted. To copy otherwise, or  
54 republish, to post on servers or to redistribute to lists, requires prior specific permission  
55 and/or a fee. Request permissions from [permissions@acm.org](mailto:permissions@acm.org).

56 © 2025 Copyright held by the owner/author(s). Publication rights licensed to ACM.  
57 ACM 0730-0301/2025/12-ART  
<https://doi.org/10.1145/nnnnnnn.nnnnnnn>

## 1.2 Binary/Gray Lighting Patterns

The most naive pattern to project onto a scene for Structured Light  
Decoding is illuminating each column. Then, the camera can take a  
picture for each column that has been illuminated, and column cor-  
respondences can be easily picked out with each picture. However,  
this requires taking as many as 4000 pictures if the user's picture  
was 4000 pixels wide, which is very impractical.

Instead, a better method is projecting a set of black-and-white  
binary or gray code stripes onto the scene. With this pattern, each  
point on the object is illuminated with a different series of stripes  
per picture, and the unique code can be picked out to identify the  
column correspondence. These methods reduce the number of images  
down to  $\lfloor \log_2 \text{Number of Column Pixels} \rfloor$ . While effective, binary  
and gray code stripe illumination both have weaknesses.

## 1.3 Global Illumination Problems

Unfortunately, when a scene is globally illuminated by a low-frequency  
pattern from long ranges, objects within the scene are subject to  
strong inter-reflections. These additional artifacts will cause certain  
parts of the scene to appear brighter in captured image, and if they  
exceed a certain threshold, they can derail the point correspondence  
decoding afterwards. In these circumstances, higher frequency light  
is more suitable. However, shining high frequency light on a scene  
is also susceptible to effects such as sub-surface scattering, where  
the projector's incident light is low-pass filtered out by nature of  
the scene and correspondences become difficult to find.

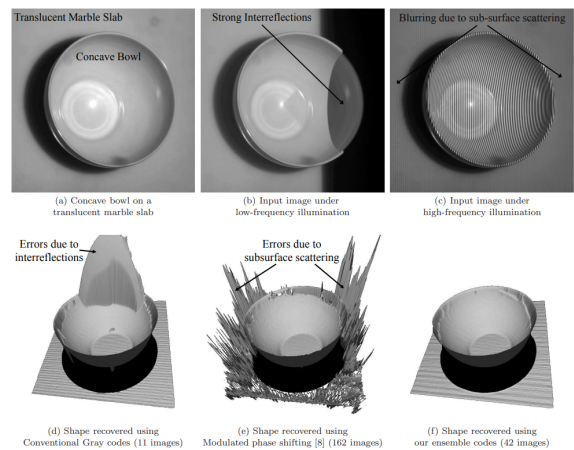


Fig. 1. Errors in reconstruction from interreflections/sub-surface scattering. From figure 7 of Paper "A Practical Approach to 3D Scanning in the Presence of Interreflections, Subsurface Scattering and Defocus"

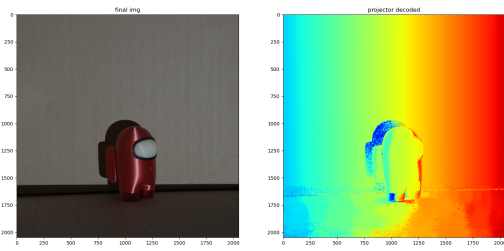
To solve this problem, Gupta et al. [2] proposed obtaining the  
low-frequency illuminated light result by applying an XOR to two  
high frequency patterns. This preserves the ability to obtain Struc-  
tured Light data without inter-reflections by shining high frequency

115 patterns all throughout, and also enables the user to obtain the  
 116 would-be low frequency direct lighting result through an additional  
 117 operator. Thus, XOR codes are a more robust way to collect ac-  
 118 curate point correspondences for 3D Structured Light. While not  
 119 entirely free of long/short range or other complex light effects, they  
 120 outperform binary and gray codes in theory.

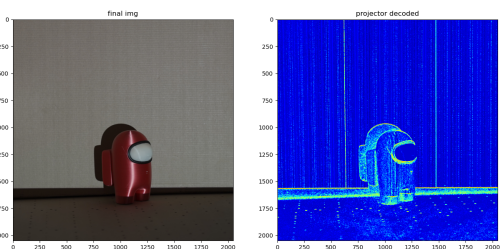
## 121 2 METHODS

### 122 2.1 Implementing Codes and Decoding

123 After securing equipment (a Sony A7III Camera, tripod, Kodak Luma  
 124 350 Projector), the first step was to create a series of binary, gray, and  
 125 XOR codes. These images were rather straightforward to generate  
 126 with numpy array functions, and for XOR, XOR-04 for used for  
 127 the first version (XOR-ing final image as the reference base plane).  
 128 Much of my algorithms for generating patterns were taken from  
 129 online procedures [3].



142 Fig. 2. Gray-Code Decoded Amongus 3D Print, from 10 gray code projec-  
 143 tions



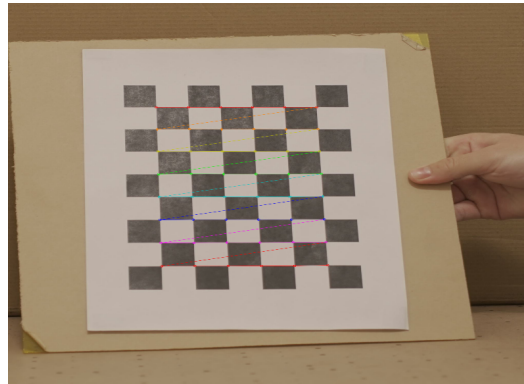
156 Fig. 3. XOR-Code Decoded Amongus 3D Print, from 10 XOR code projec-  
 157 tions

159 Decoding was equally straightforward. The scene was chosen to  
 160 be of an image 2048 x 2048 pixel size, because increasing the columns  
 161 any larger would lead to increasingly inaccurate decodings (short-  
 162 range effects). After capturing 10 images of the scene, the images  
 163 were stacked and codes were extracted per-pixel. The threshold for  
 164 determining a corresponding '0' or '1' in each pixel position across  
 165 the stack of images was simple the per-pixel mean of the stack.

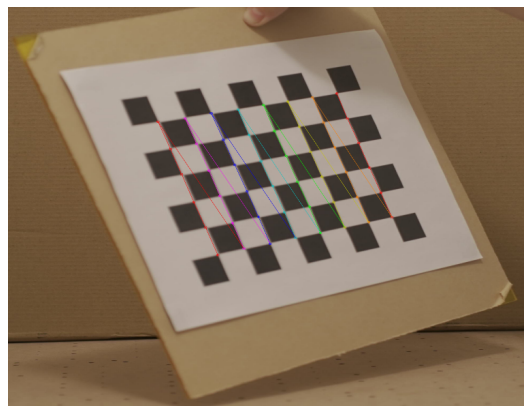
### 166 2.2 Camera Calibration

168 To use stereo triangulation, the camera's intrinsic and extrinsic  
 169 parameters needed to be found. Finding the camera's intrinsic pa-  
 170 rameters involved simply capturing images of the 9x7 chessboard

172 from a series of different poses and then using Zhang's method [4]  
 173 via cv2.calibrateCamera to extract the intrinsic and distortion.  
 174 This process actually took significant amounts of time and re-doing,  
 175 especially after a belated realization that cropping an image would  
 176 alter the camera's respective  $f$  parameters.



188 Fig. 4. Camera Calibration Image 1



199 Fig. 5. Camera Calibration Image 2

### 213 2.3 Projector Calibration

215 Another requirement that was needed for stereo triangulation was  
 216 the projector's intrinsic and extrinsic parameters. Ultimatley, the  
 217 method used was from Daniel Moreno and Gabriel Taubin's pro-  
 218 projector calibration proposal [4]. Their paper proposed the following  
 219 method: after calculating the camera's intrinsic parameters, pro-  
 220 projector calibration can be done by projecting all gray code patterns  
 221 onto a chessboard at various poses (in this case, five were used).  
 222 Then, to approximate the projector's intrinsic matrix, the row/col  
 223 of each chessboard corner that were captured by the camera could  
 224 be mapped by homography to the gray-decoded image. Instead of a  
 225 global homography, however, the process was made more robust  
 226 by capturing individual homographies in a patch neighborhood for  
 227 each corner. If a homography was found successfully, it could be

**ALGORITHM 1:** Projector Calibration

---

```

229 Input: Chessboard Images  $I_{\text{chessboards}}$ , decoded gray-code image
230       $I_{\text{decoded}}$ , Camera's Intrinsic Matrix and Distortion
231      Parameters  $K_c, d_c$ 
232
233 Output: Projector's Intrinsic Matrix, Projector's Distortion
234      Parameters  $K_p, d_p$ 
235 ;
236 for each image  $I$  in  $I_{\text{chessboards}}$  do
237      $\text{Corners}_c = \text{findChessboardCorners}(I, K_c, d_c)$ 
238     for each corner $c$  in  $\text{Corners}_c$  do
239        $\text{patch} = \text{get_neighborhood}(\text{corner})$ 
240       for  $p_x, p_y$  in  $\text{patch}$  do
241         if  $\text{decoded}[p_y] - p_x < \text{tolerance}$  then
242            $pp_x = \text{decoded}[p_x]$   $pp_y = y$ 
243         end
244       end
245        $H = \text{getHomography}(\text{all } pp_x, \text{all } pp_y)$ 
246       if  $H$  exists then
247          $\text{corner}_p = H \times \text{corner}_c$ 
248          $\text{Corners}_p.append(\text{corner}_p)$ 
249       end
250     end
251   end
252    $K_p, d_p = \text{calibrateCamera}(\text{Corners}_c, \text{Corners}_p, I_{\text{chessboards}})$ 
253

```

---

used to map the camera's captured chessboard corner to the projector's decoded version to form a new point, which then could be fed into `cv2.calibrateCamera` to find the projector's intrinsic matrix and distortion parameters.

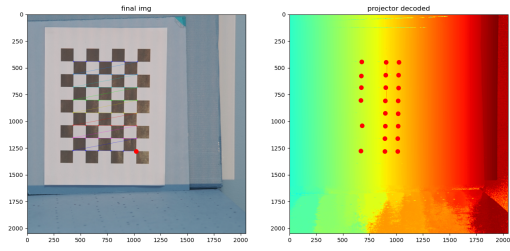


Fig. 6. Checkerboard Pose 1, Projector Calibration Corner Mapping via patch neighborhood homographies

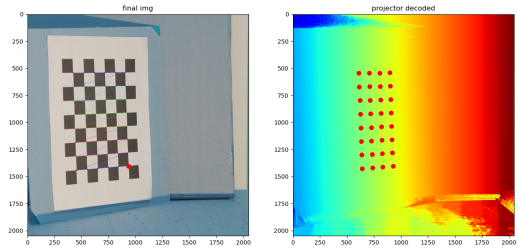


Fig. 7. Checkerboard Pose 2, Projector Calibration Corner Mapping

Then, after finding intrinsic/distortion parameters for both the camera and projector, the extrinsic Rotation and Translation matrices from one to the other were found with a stereo calibration function call (`cv2.stereoCalibrate`).

This process was easily the most arduous of the final project, and had to be redone many times due to numerous situational lighting problems or algorithm issues.

## 2.4 Triangulation

After calculating the camera's Intrinsic Matrix and distortion  $K_c, d_c$ , the projector's Intrinsic Matrix and distortion  $K_p, d_p$ , and the Camera to Projector stereo rotation and translation vectors  $R, T$ , solving the triangulation problem becomes extraordinarily simple. First, we back-project the camera point with its perspective matrix  $K_c[I|0]$  and distortion parameters, where  $I$  is a  $3 \times 3$  identity matrix. Then, we similarly back-project the same point with the projector perspective matrix  $K_p[R|t]$  and its own distortion parameters, and measure the intersection. The  $z$  value found at that intersection corresponds to the depth from the stereo pair. By performing this operation with each detected point correspondence found in the Structured Light decoded image, a point cloud can be formed.

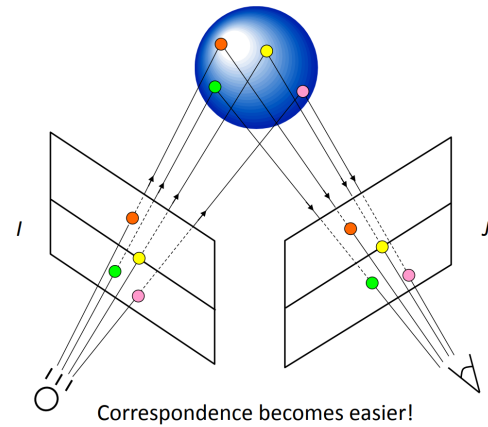


Fig. 8. Setup Picture 1

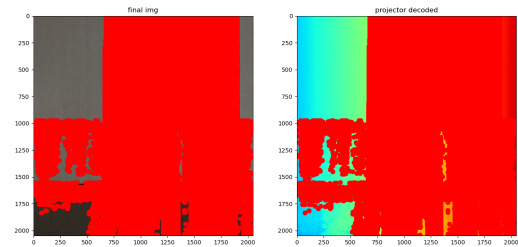
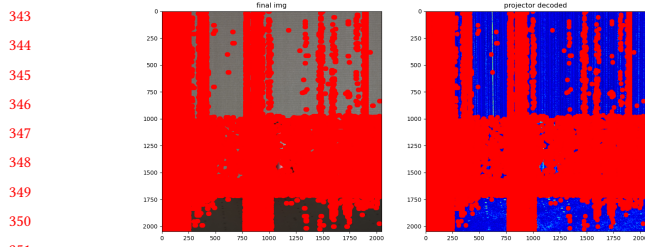


Fig. 9. Decoded Correspondence Points found in Gray code patterns on Among Us



343  
344  
345  
346  
347  
348  
349  
350  
351  
352  
353  
354  
355  
356 Fig. 10. Decoded Correspondence Points found in XOR patterns on Among  
Us

### 3 EXPERIMENTAL EVALUATION



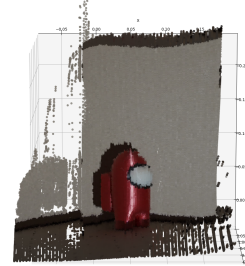
357  
358  
359  
360  
361  
362  
363  
364  
365  
366 Fig. 11. Setup Picture 1



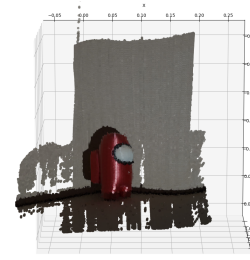
368  
369  
370  
371  
372  
373  
374  
375  
376  
377  
378  
379  
380  
381  
382  
383  
384  
385  
386  
387  
388 Fig. 12. Setup Picture 2

390 The procedure above was done with gray codes, binary codes, and  
391 XOR codes. While XOR codes were expected to produce the best  
392 result, due to projector resolution difficulties, they performed relatively  
393 weaker compared to the gray code and binary code results.  
394 However, what *can* be seen of their shape is more promising in  
395 regards to removing inter-reflection artifacts, as expected. Unfortunately,  
396 the time before the final project deadline was too tight to  
397 implement the truly robust method in Gupta et al's paper, where a  
398 combination of low-frequency gray codes of two types and XOR-2,  
399

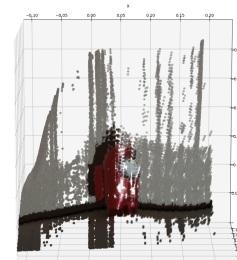
400 XOR-4 codes could be used to cross-verify and produce the best  
401 result.



402  
403  
404  
405  
406  
407  
408  
409  
410  
411  
412  
413  
414 Fig. 13. Among us, projected with Binary Codes



420  
421  
422  
423  
424  
425  
426  
427  
428  
429  
430 Fig. 14. Among us, projected with Gray Codes



431  
432  
433  
434  
435  
436  
437  
438  
439  
440  
441  
442  
443  
444  
445  
446 Fig. 15. Among us, projected with XOR Codes

447  
448  
449  
450  
451  
452  
453  
454  
455 Here, clearly, the XOR code did not overwhelmingly outperform the gray and binary codes as anticipated. However, if one examines closely, I think it handles the shiny 3D-printed material specularity better and captures the shape with less distortion in various portions. The same goes for the Waddle Dee and Kombucha Bottle below.

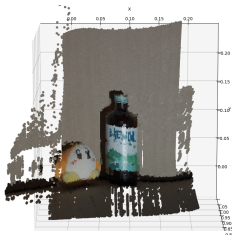


Fig. 16. Waddle Dee and Kombucha Bottle, projected with Gray Codes

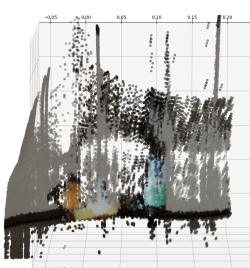


Fig. 17. Waddle Dee and Kombucha Bottle, projected with XOR Codes

## 4 POTENTIAL DIRECTIONS

Because camera and projector calibration took an extensive portion of time, it was difficult to attempt more ambitious Structured Light code patterns. Other codes include Parsa et al's proposed À La Carte Structured Light Patterns [5], where image data can be fed into a ZNCC (zero normalized cross correlation) and a maximum likelihood objective function can be formed to find optimal structured light patterns for a given noisy image. Like what was mentioned above, another avenue that would have been promising to explore would be to have implemented the minimum gray stripe-width codes and XOR-2 codes, and create a self-verifying pipeline resistant to low-range and high-range light effects.

## 5 CONCLUSIONS

Structured light offers an efficient, relatively cheap, and accurate method for 3D scene reconstruction. This project explored various approaches to structured light, including binary codes, gray codes, and XOR codes. While XOR codes were expected to outperform others due to their robustness to global illumination issues, projector resolution limitations hindered their performance in this experiment.

While the implementations of algorithms for camera and projector calibration, along with triangulation to create a 3D point cloud were successful, the camera and projector calibration proved to be a time-consuming bottleneck. After having learned first-hand how to calibrate, I'm sure that I could go further with the other pursuits mentioned above if I had more time. Examining À La Carte structured light patterns or implementing minimum gray stripe-width codes with XOR codes could lead to a more robust system resistant to various light effects. Additionally, more complex structured

light code patterns or real time would have been also wonderful to implement.

## 6 REFERENCES

Digital Michelangelo Project [Levoy 1999] 514  
 A Practical Approach to 3D Scanning in the Presence of Interreflections, Subsurface Scattering and Defocus (where XOR projection patterns were proposed) [Gupta et al. 2013] 515  
 À La Carte Structured Light [Mirdehghan et al. 2018] 516  
 Simple, Accurate, and Robust Projector-Camera Calibration [Moreno and Taubin 2012] 517  
 Helpful Repository on Obtaining Generating Pattern Code 518  
<https://github.com/elerac/structuredlight> 519  
 Taubin G., Moreno D., Lanman D. 2014 Course on 3D Structured Light Scanning [PowerPoint presentation], Brown University 520  
 Srinivasa et al., Nayar et al., 2016 16823 Structured Light 3D Scanning Lecture [PowerPoint presentation], Carnegie Mellon Univ 521  
 Gkioulekas, I. 2017 15463 Computational Photography Course Lecture 27 Structured Light [PowerPoint presentation], Carnegie Mellon Univ 522  
 Procam Repository, which implements the Projector Calibration source mentioned in paper: Simple, Accurate, and Robust Projector-Camera Calibration 523  
<https://github.com/kamino410/procamcalibration> 524

## REFERENCES

Mohit Gupta, Amit Agrawal, Ashok Veeraraghavan, and Srinivasa G. Narasimhan. 2013. A Practical Approach to 3D Scanning in the Presence of Interreflections, Subsurface Scattering and Defocus. *Int. J. Comput. Vision* 102, 1–3 (March 2013), 33–55. <https://doi.org/10.1007/s11263-012-0554-3> 525  
 M. Levoy. 1999. The digital Michelangelo project. In *Second International Conference on 3-D Digital Imaging and Modeling (Cat. No.PR00062)*. 2–11. <https://doi.org/10.1109/IM.1999.805329> 526  
 Parsa Mirdehghan, Wenzheng Chen, and Kiriakos N. Kutulakos. 2018. Optimal Structured Light à la Carte. In *2018 IEEE/CVF Conference on Computer Vision and Pattern Recognition*. 6248–6257. <https://doi.org/10.1109/CVPR.2018.00654> 527  
 Daniel Moreno and Gabriel Taubin. 2012. Simple, Accurate, and Robust Projector-Camera Calibration. In *2012 Second International Conference on 3D Imaging, Modeling, Processing, Visualization Transmission*. 464–471. <https://doi.org/10.1109/3DIMPT.2012.77> 528